DIGITAL ACCESS TO SCHOLARSHIP AT HARVARD

A Muscle's Force Depends on the Recruitment Patterns of Its Fibers

Citation	Wakeling, James M., Sabrina S. M. Lee, Allison S. Arnold, Maria Boef Miara, and Andrew A. Biewener. 2012. "A Muscle's Force Depends on the Recruitment Patterns of Its Fibers." Annals of Biomedical Engineering 40 (8) (August): 1708–1720.
Published Version	doi:10.1007/s10439-012-0531-6
Accessed	February 19, 2015 2:05:09 PM EST
Citable Link	http://nrs.harvard.edu/urn-3:HUL.InstRepos:11949244
Terms of Use	This article was downloaded from Harvard University's DASH repository, and is made available under the terms and conditions applicable to Open Access Policy Articles, as set forth at http://nrs.harvard.edu/urn-3:HUL.InstRepos:dash.current.terms-of-use#OAP

(Article begins on next page)

A muscle's force depends on the recruitment patterns of its fibres

James M. Wakeling[1], Sabrina S.M. Lee[1], Allison Arnold[2], Maria de Boef Miara[2] and Andrew

Biewener[2].

[1]Department of Biomedical Physiology and Kinesiology,

Simon Fraser University,

Burnaby, BC, Canada

[2]Department of Organismic and Evolutionary Biology,

Harvard University,

Concord Field Station,

Bedford, MA 01730

ORIGINAL VERSION 6440 words

2. Abstract

Biomechanical models of whole muscles typically assume that the muscle generates force as a scaled-up muscle fibre. However, muscles are comprised of motor units that have different intrinsic properties and that can be activated at different times. This study tested whether a muscle model comprised of motor units that could be independently activated resulted in more accurate predictions of force than traditional Hill-type models. Forces predicted by the models were evaluated by direct comparison with the muscle forces measured *in situ* from the gastrocnemii in goats. The muscle was stimulated tetanically at a range of frequencies, muscle fibre strains were measured using sonomicrometry and the activation patterns of the different types of motor unit were calculated from electromyographic recordings. Activation patterns were input into five different muscle models. Four models were traditional Hill-type models with different intrinsic speeds and fibre-type properties. The fifth model incorporated differential groups of fast and slow motor units. Muscle performance depends on the recruitment of different motor units within the muscle. For all goats, muscles and stimulation frequencies the differential model resulted in the best predictions of muscle force.

Key words: muscle model, sonomicrometry, EMG

3. Introduction

Muscle models, in combination with electromyographic (EMG) recordings of muscle activity, are key components of dynamic simulations used to investigate musculoskeletal function during movement (e.g., Buchanan et al. 2004). The forces that a muscle produces during contraction can be estimated using phenomenological, Hill-based relations that describe how the force is influenced by factors including the muscle's length, velocity, and activation (e.g. van Leeuwen, 1992; Epstein and Herzog, 1998). However, Hill-type models commonly implemented in simulations of movement have limitations. For example, whole muscles are typically represented as scaled-up fibres, driven by a single contractile element with average biochemical and mechanical properties. Estimates of the muscle forces derived from such models have rarely been validated, in part, due to the challenges associated with measuring the forces during natural behaviors. This is particularly the case involving human muscles. Some recent studies have been made to validate scaled length-tension relationships for whole muscles (e.g., Winters et al., 2011), the simulated 3D geometry of muscles during contraction (Böl et al. 2011), and some experiments have been done to qualitatively confirm the actions of select muscles predicted by simulations (e.g. Hernandez et al., 2010). However, the accuracy with which traditional, Hill-type models predict muscle forces during *in vivo* activities remains untested.

Recent studies of motor unit recruitment suggest that existing Hill-type models may not adequately capture the complex relations between motor unit recruitment within a muscle, the EMG signals generated, and the resulting forces developed (e.g., Hodson-Tole and Wakeling, 2009). Most mammalian skeletal muscles contain mixed populations of different muscle fibre types. The contractile properties of muscle fibres vary between fibre types (e.g. Burke et al. 1971; Bottinelli and Reggiani, 2000), so it is likely that the force developed by a whole muscle depends on the recruitment patterns and contractile properties of the different fibres within it

(Fuglevand et al. 1993). Some models have included different fibre-type properties, however these have been limted to the simulation of isometric contractions (Fuglevand et al. 1993; Böl et al. 2011). However, recruiting different muscle fibre-types is of particular functional importance during dynamic movements (Hodson-Tole and Wakeling, 2009). Most existing muscle models that are used to simulate gait and movements assume that the contractile function of a whole muscle can be scaled up from a single fiber with little, or no regard for the patterns of motor unit recruitment or the properties of the different motor units recruited.

This study used a modified Hill-based approach to examine how the contributions of different constituent fibres influence the mechanical output of whole muscle. Specifically, we hypothesized that the fluctuations in force that occur during unfused and fused tetanic contractions would be better predicted by a model that activated fast and slow motor units independently than by a model that activated the whole muscle as a homogeneous block. Five different models were used to predict the forces generated during *in situ* nerve stimulation experiments. Four of the models were traditional Hill-type models that were assigned different fibre-type proportions, intrinsic activation dynamics, and force-velocity relations (Hill, 1970; Winters and Stark, 1988; Zajac, 1989). A fifth model was developed where contractile elements of different fibre types could be activated independently. The activation patterns to drive this fifth model were derived from the fast and slow components of the EMG signals recorded from these muscles (Lee et al. 2011). Performance of the models was evaluated in a system where the muscle forces could be measured directly, and this was not possible in man; therefore, the models were tested against the measured muscle forces from a mammalian model, the goat. Whilst the models are tested against measurements of fixed length contractions of the muscle-tendon unit, they are set-up to be just as suitable for dynamic contractions *in vivo*.

4. Materials and methods

Muscle models were tested using physiological data measured *in situ* from five goats (*Capra hircus*; age 17.2 ± 52 months; mass 25.4 ± 1.7 kg, mean ± s.e.m.) at Harvard University's Concord Field Station. All surgical and testing procedures followed IACUC approval.

Nerve stimulation experiments

The data used to test the models form part of a larger study; full details for the three-day procedures have been reported elsewhere (Lee et al. 2011). In brief, on day one the medial and lateral gastrocnemius muscles (MG and LG) were each instrumented with bipolar silver-wire EMG electrodes (0.1 mm enamel insulated silver: California Fine Wire, Grover Beach, CA) and a pair of 2 mm sonomicrometry crystals (Sonometrics Inc., London, ON, Canada) aligned along the fascicle direction within the muscle belly: sonomicrometry is a technique for measuring fascicle lengths based on the transmission time of acoustic signals between the piezoelectric crystals A custom-fabricated "E"-shaped tendon buckle was also attached to the common gastrocnemius tendon (McGuigan et al. 2009). *In vivo* measures of locomotor activity were recorded on day two. On day three, a second surgical procedure was done, and *in situ* nerve stimulation experiments were performed. Tri-polar nerve cuffs were placed around the branches of the tibial nerve that innervate the MG and LG. A second "E"-shaped tendon buckle was mounted on either the medial or lateral portion of the tendon, proximal to the common buckle, by separating tendons by blunt dissection and more distally by separating the collagen fibrils with a scalpel. The goat was then placed in a stereotactic frame whereby the femur and tibia were secured with bone pins and the foot was strapped to a plate that allowed extension at the ankle. The goat was maintained at 0.5-1.0 % isoflurane anaesthesia for the duration of the testing. The goat was ultimately euthanized with an intravenous injection of sodium pentobarbitol.

Contractile measurements were made on the MG and then the LG with nerve stimulations

applied during *in situ* tests. A heating pad was used to maintain a constant muscle temperature of about 34 ± 0.7 °C (mean $\pm$ s.d., $N=5$). Initial investigation determined the threshold stimulus voltage that resulted in the greatest twitch force. Subsequent twitches were stimulated using a 1.5 times threshold pulse that was 2 ms in duration. The frame allowed the ankle flexion-extension angle to be varied, but it was held fixed for each contraction. Each test was for the limb held fixed in the stereotactic frame, and thus resulted in contractions that were isometric for the muscle-tendon unit of the MG and LG. The active and passive force-length relationship was measured using tetanic stimulation (at 40 Hz stimulation frequency) for a range of different ankle angles (and thus muscle lengths) that were set within the stereotactic frame. The ankle was subsequently fixed at the angle that resulted in maximum tetanic force at the tendon. A series of tetanic contractions were then measured at stimulation frequencies of 5, 10, 20 and 40 Hz. The 20 and 40 Hz tests were no more than 0.5 seconds in length, and a 2-minute rest was given between all tetanic contractions to minimize muscle fatigue.

Analog signals were conditioned for the EMG (P511J amplifiers, Grass, West Warwick, RI), sonomicrometry (model 120-1000, Triton Technology Inc, San Diego, CA), and tendon forces (bridge amplifier, Vishay 2120, Micro-Measurements, Raleigh, NC). Analog signals were acquired on a 16-bit analog-to-digital convertor (NI 6259, National Instruments, Austin, TX), and recorded at a 5000 Hz sample rate. Fascicle length changes measured via sonomicrometry were corrected for the sound velocity of muscle at 34 °C and the offset introduced by the epoxy of the lens of each crystal as described in Gillis and Biewener (2005).

Muscle contractile parameters

Contractile characteristics of the muscles, including activation, force-length and maximum intrinsic speed were estimated from the experimental data. The EMG signal contains time-varying information about the motor recruitment strategies, that is encoded by frequency

properties of the signal. The intensity of the EMG signals was calculated using wavelet analysis, a time-frequency decomposition technique that has been described extensively by, for example, Lee et al. (2011), Wakeling et al. (2002) and von Tscharner (2000). The total intensity was calculated across the frequency band 101-1857 Hz using a filter-bank of non-linearly scaled wavelets and is a close approximation to the power of the signal (Lee et al. 2011). The intensities of the EMG across high- (240-423 Hz) and low- (82-247 Hz) frequency bands that identify the myoelectric activity from faster and slower motor units, respectively, were calculated from specific wavelets that had been optimized to the EMG intensity spectra from these motor units in the goat (Hodson-Tole and Wakeling, 2007; Lee et al. 2011).

The activation level is a representation of the capacity of the muscle to actively develop force, and reflects the Ca^{2+} concentration within the sarcoplasm. EMG intensities were converted to muscle activations using transfer functions formed by sets of three first-order differential equations that have previously been characterized for these goats (Lee et al. 2011). These transfer functions were validated by correlating the predicted active state to the measured isometric force (from the same data as in this study: r=0.98-0.99; Lee et al. 2011), The transfer functions incorporate both a timing offset to accommodate electromechanical delay, and coupled differential equations to describe the differing activation and deactivation rates and the persistence of the rise in activation after the action potentials in the EMG have passed. Muscle activity as a function of time, denoted by $a(t)$, was calculated for the whole muscle and for the fast- and slow- motor units from their EMG intensities using methods that we have previously described (Lee et al. 2011). The muscle activations were normalized, $\hat{a}(t)$, to the maximum activity of the whole muscle that occurred across all tetanic contractions.

Force-length properties were determined for these goats as a function of fascicle strain. The resting fascicle length was defined as the passive fascicle length at the ankle angle that

yielded maximum force. Force-length properties, $\hat{F}(l)$, were normalized to the maximum isometric force and were averaged for the five goats.

The maximum unloaded shortening velocities, v_0 (muscle lengths s^{-1}), were estimated for the fast- and slow fibres in two ways. First, the following relation for locomotor muscles in terrestrial species was used, derived from a literature survey of 59 species from 88 papers ($r^2 = 0.75$; Hodson-Tole and Wakeling, personal communication):

$$v_0 = 71.1\tau_a^{-0.74}. \tag{1}$$

τ_a is the time to maximum twitch force (ms), and was estimated for these goats as 52.9 and 98.6 ms for the fast- and slow-fibres, respectively (Lee et al. 2011). This relation yielded v_0 values of 3.59 and 2.74 s^{-1} for the fast and slow fibres, respectively. A variant of the muscle models was evaluated using faster v_0 to test the sensitivity of the models to the choice of v_0. No data currently exist for v_0 for larger mammals at physiological temperatures; however, v_0 for the mouse, rat and cat at physiological temperatures range between 4.8 – 7.3 s^{-1} for slow fibres (Askew and Marsh, 1998; Close, 1964; Spector et al. 1980) and 9.2 – 24.2 s^{-1} for faster fibres (Askew and Marsh, 1997; Luff, 1981; Close, 1965; Ranatunga, 1982; Close, 1964; Close and Luff, 1974; Luff, 1975; Spector et al. 1980; Buller et al. 1987). Larger animals have lower v_0 (Close, 1972; Toniolo et al. 2004), and v_0 would be slightly less at the depressed temperature of 34 °C during these *in situ* experiments. Therefore, we additionally selected v_0 values of 5 and 10 s^{-1} for the slow and fast fibres, respectively. For the purposes of this study, fibre velocity was measured relative to the passive fibre length that resulted in the maximum isometric force, and thus velocity was equivalent to the fibre strain rate.

Muscle models

Five muscle models were used to estimate the muscle force (see summary of parameters

in Tables 1 and 2). Models A-D are described in the following sections, but they shared the following features. The activation state was determined from the total EMG intensity, and the total muscle force F_m was given by:

$$F_m = c_1[\hat{F}_f + \hat{F}_p(l)]\cos\beta, \tag{2}$$

where $\hat{F}_f$ is the active component of the muscle fibre force, $\hat{F}_p(l)$ is the passive component of the force-length relationship, β is the pennation angle (assumed constant for the isometric contractions in this study), and c_1 scaled the fibre force to the whole muscle force (Otten, 1987b; van Leeuwen, 1992; Askew and Marsh, 1998).

Models (A-C) were similar to those currently used for biomechanical simulations of human and animal movement. In these models the normalized, active component of the muscle fibre force $\hat{F}_f$ was given by the expression (van Leeuwen, 1992):

$$\hat{F}_f = \hat{a}(t)\hat{F}_a(l)\hat{F}(v), \tag{3}$$

where $\hat{a}(t)$ is the time-varying level of activation, normalized to a maximum of 1, $\hat{F}_a(l)$ is the active force-length relationship, normalized to a maximum of 1. During contractions the fascicle lengths fluctuate and so both length, l, and velocity, v, are time-varying in addition to $\hat{a}(t)$.

When a muscle fibre contracts its force depends on the contraction speed with the force diminishing to zero for very rapid contractions, and increasing to 150% its isometric levels for lengthening contractions: The force-velocity relationship, $\hat{F}(v)$ was normalized to an isometric value of 1 and was given by:

$$\hat{F}(v) = \frac{(1 - \dfrac{v}{v_0})}{(1 + \dfrac{v}{v_0 k})} \qquad \text{for } v \leq 0 \tag{4}$$

$$\hat{F}(v) = 1.5 - 0.5 \left[\frac{(1 - \dfrac{v}{v_0})}{(1 - \dfrac{7.56v}{v_0 k})} \right] \quad \text{for } v > 0 \tag{5}$$

where v is the contractile velocity of the fibre and v_0 is its maximum intrinsic speed (van Leeuwen, 1992; Hodson-Tole and Wakeling, 2010). Constant k describes the curvature of the force-velocity curve and depends on muscle fiber type (Otten, 1987). The curvature for the faster fibers of locomotor muscles in terrestrial species (k=0.29) is significantly flatter than for slower fibres (k=0.18), as determined from a literature survey of 59 species from 88 papers (Hodson-Tole and Wakeling, personal communication). Values of v_0 and k were chosen for the different muscle models as follows:

Homogeneous model A assumed that the muscles contained fibers with homogeneous properties. v_0 was taken from the maximum intrinsic speeds of the different fiber types weighted by their fractional cross-sectional areas. The curvature k was assumed to be the same for all fibres, and was assigned an intermediate value between the fast and slow fiber limits, following rationale in Zajac (1989):

$$k = k_{\text{slow}} + (k_{\text{fast}} - k_{\text{slow}})p \tag{6}$$

where p is the fractional area occupied by the fast muscle fibers (Winters and Stark, 1988). Because p is not yet known for the goat, we analyzed two variants of the models, with p=0.75 and p=0.5 to bracket the range of fast-fibre proportions in the gastrocnemii reported from six different species (Ariano et al. 1973; Johnson et al. 1973).

Hybrid model B was the same as homogeneous model A except that v_0 represented the fastest fibers and k was calculated from the composite force-velocity relation taken from a combination of fast and slow fibres with forces proportional to their fractional fibre area following Hill

(1970). This assumption resulted in a greater curvature than calculated using equation 5.

Orderly recruitment model C assumed that as the level of activation increases, the active muscle takes the intrinsic properties of progressively faster fibre types. These ideas stem from the classic observations of orderly recruitment during steady stretch reflexes (Henneman et al., 1974) and follow previous approaches (van Soest and Bobbert, 1993; Umberger et al. 2003), but here v_0 was activation dependent and was scaled to equal that of the slowest fibres at the lowest (near zero) activation levels:

$$v_0 = v_{0,\text{slow}} + (v_{0,\text{fast}} - v_{0,\text{slow}})\hat{a}(t) \tag{7}$$

For this model, k was calculated using equation 6, and the muscle fibre force F_f was calculated using equation 3.

Reverse recruitment model D assumed that as the level of activation increases, the active muscle takes the characteristics of progressively slower fiber types. This may be appropriate during direct electrical stimulation to the nerve where the larger diameter axons from the faster motor units are the most excitable (Tanner, 1962; Solomonow, 1984), but is not expected to occur *in vivo*. For this reverse recruitment model, k was calculated using equation 6 and v_0 was activation dependent in an opposite manner to model C:

$$v_0 = v_{0,\text{fast}} - (v_{0,\text{fast}} - v_{0,\text{slow}})\hat{a}(t) \tag{8}$$

Differential recruitment model E contained fast and slow contractile elements in parallel that could be differentially activated. The activation levels for the fast and slow elements, $\hat{a}_{\text{fast}}(t)$ and $\hat{a}_{\text{slow}}(t)$, respectively, were determined from the EMG intensity at the high- and low- frequency bands (Lee et al. 2011). The total muscle force F_m for this model was given by:

$$F_m = c_1\left[c_2\hat{F}_{f,\text{fast}} + c_3\hat{F}_{f,\text{slow}} + \hat{F}_p(l)\right]\cos\beta \quad F_m = c_1\left[c_2 F_{f,\text{fast}} + c_3 F_{f,\text{slow}} + F_p(l)\right]\cos\beta \tag{9}$$

where c_2 and c_3 scaled the relative contribution of the fast and slow elements, respectively, and

$\hat{F}_{f,fast}$ and $\hat{F}_{f,slow}$ are the normalized forces from fast and slow fibres, respectively, as determined

from Equation 2 using fibre-specific values of $\hat{a}(t)$, v_0 and k (Table 2), The ratio c_2/c_3 partially

reflects the lower EMG intensities that would be expected from action potentials with higher

spectral frequencies, and a value of 10 was used.

Statistics

The models were run 800 times (5 models × 5 goats × 2 muscles × 4 stimulation frequencies × 2

choices of p × 2 sets of v_0). For each run, the coefficient of determination, r^2, was calculated

between the predicted force and the measured tendon force, and these data were used as the

dependent variable in an ANOVA. Model type, goat (random), muscle, stimulation frequency,

fibre-type proportion and selection of v_0 were used as factors. Differences were considered

significant at the $\alpha=0.05$ level. Values are reported as mean ± s.e.m..

5. Results

All models captured the salient features of the measured muscle forces, generating

oscillating forces at the low (5 – 10 Hz) stimulation frequencies and fused tetanic contractions

for the highest (40 Hz) stimulation frequency (Figs. 1-3). However, the models varied in their

ability to reconstruct the force traces, particularly the force rise and the force relaxation. These

differences were most apparent for the low frequency stimulations (5 Hz) where the rise and fall

characteristics play a major role in the force trace. The models generally performed better for the

higher stimulation frequencies (Fig. 2). The differential model E performed best for all

stimulation frequencies and both muscles (Figs. 4, 5).

Model E accounted for fluctuations in the EMG intensity from the fast and slow motor

units (Fig. 4), and this modification improved its performance. During contractions, we measured oscillations in both fascicle length and whole muscle force. The fascicles oscillated in length as they worked against the series compliance of the tissue (internal and external tendon), showing substantial variations in strain (standard deviation 0.075) and shortening strain rate (standard deviation 0.704 s^{-1}) across trials. The peak twitch forces for the 5 Hz stimulus trains, for instance, showed no systematic trend over the course of the stimulus (linear regression, $p=0.728$) and had a standard deviation of 9.5% (from the second peak onwards, relative to the mean peak force). Considerable and independent fluctuations also occurred in the intensity of the MU action potentials in the high- and low-frequency bands as determined from wavelet analysis (Fig. 6B), though the MU action potentials in each train had similar amplitudes (Fig. 6A). The time course of the activation levels similarly varied between the different types of motor unit; in the example shown in Fig. 6C, the fast MU activation level fluctuated with each stimulus, and gradually decreased over the contraction, whereas the slow MU activation level increased gradually over the course of the contraction.

ANOVA showed that there were significant differences in the outputs from the different models, and that model outputs were dependent on the choice of v_0, muscle, stimulation frequency, goat and most importantly the type of model used ($p<0.001$; Fig. 5). Selecting v_0 of 5 and 10 s^{-1} rather than the slower values estimated for the goat resulted in a better reconstruction: $r^2 = 0.843 \pm 0.007$ as compared to 0.758 ± 0.009 (mean ± s.e.m., $N = 400$ each group). The models generated a better fit for the LG muscle than for the MG muscle: $r^2 = 0.836 \pm 0.007$ as compared to 0.766 ± 0.009 (mean ± s.e.m., $N = 400$ each group). The fibre-type proportion selected for the model did not significantly influence the model outputs.

6. Discussion

Activation parameters to drive muscle models

This study was based on the premise that EMG signals from the muscles contain information about the motor recruitment patterns, and that extracting and using this information would result in better muscle models. Extracting this information from an EMG can prove challenging both in the experimental design and signal analysis, and different approaches have yielded different successes in resolving such information (eg. Farina et al. 2002; Wakeling et al. 2002, 2009). The specific approach is this study used fine-wire EMG and has been previously developed and validated for these goat muscles (Lee et al. 2011). The main difference between the differential model E and the models A-D is that the differential model is driven by the fast-slow motor unit recruitment information that is encoded in the EMG. The fact that the differential model resulted in the best performance (Fig. 4) is a good indication that the motor recruitment information was encoded in the EMG, it was successfully resolved, and it is an important determinate of the mechanical function of the muscles.

All models in this study used a three-step function to estimate the activation state from the EMG intensity (Lee et al. 2011), and this differs from previous studies that have used a single first-order differential equation (eg. Zajac, 1989). Whilst the purpose of this study was not to evaluate different methods for calculating the active state of the muscle, Fig. 2 shows that the predicted muscle force is influenced by how activation is calculated. Using a single bilinear first-order differential equation to estimate activation only allows the activation to increase while the EMG intensity is positive (Zajac, 1989; Fig. 2B; all other parameters being the same as model A). This is limiting, since action potentials may exist for about 3 ms while the force rise during twitch can last up to 100 ms (Lee et al. 2011). Prolonged activation, persisting after the action potential has decayed, occurred using the 3-step transfer functions in this study (Models A-E; Lee et al. 2011), and this resulted in a substantial improvement in the predicted muscle forces

(Fig. 2B).

The models in this study assumed that the muscle activation, force-velocity and force-length properties were independent, typical of Hill-type models. However, it is known that activation depends on muscle length (Close, 1972; Stephenson and Wendt, 1984; Balnave and Allen, 1996), and that activation in turn affects the force-length and force-velocity properties (Rack and Westerbury, 1969; Roszek et al. 1994; Brown et al. 1999). Additionally, muscle forces are modulated by history-dependent effects (Rassier et al. 2003) and fatigue (Edwards, 1981). In future, the models presented here could be further refined to incorporate these coupling and history-dependent effects. The results from this study demonstrate how muscle model predictions depend on the mechanics of the active motor units.

Within the models used in this study, a number of scaling constants have been used. Constant c_1 was used for all models, (equations 2 and 9), and serves to scale the force from a normalized value to the actual force from the muscle. c_1 can be considered as the maximum isometric force that the muscle can develop. The evaluation of the models was based on correlation analysis that is independent of the scale of the measured and predicted forces, and thus the choice of c_1 does not affect the conclusions. Constants c_2 and c_3 scale the relative contributions from the fast- and slow-components of the differential model E (equation 9). A number of factors would contribute to the ratio c_2/c_3, and these include the fibre-type proportion within the muscle, the proximity of the different types of fibre type to the recording electrodes, and the transfer of action potential magnitude to the predicted active state of the different types of motor unit. Due to uncertainty in the former two factors, the selection of c_2/c_3 was based on some simplifying assumptions about the transfer of action potential amplitude. Faster motor units have action potential conduction velocities and thus EMG frequencies typically 2-3 times greater than slower motor units (Wakeling et al. 2002; Wakeling and Syme, 2002; Hodson-Tole and

Wakeling, 2009; Lee et al. 2011). If an action potential from a faster motor unit was considered as a single cycle of a pure frequency, its Fourier transform would be 1/2 to 1/3 in magnitude, and it would have 1/4 to 1/9 the power or intensity. Thus the intensity of the high-frequency signal from the faster motor units would need to be scaled by a factor of up to 9 to make it equivalent to a measure of action potentials. We have used a general scale factor of 10 for c_2/c_3 to accommodate this effect. Understanding this ratio in more detail would clearly be an avenue for future investigation. It is possible that misrepresentation of this ratio would contribute to the statistical finding that fibre-type proportion did not have a significant effect on the model performances (Fig. 5), as this is one of the factors that may influence c_2/c_3.

Intrinsic properties of the modelled fibres

The five muscle models differed in their force-velocity relations and in how the active state of the muscle fibres was calculated (Fig. 5). These differences statistically influenced the accuracy of the predictions of whole muscle force. Force-velocity relations depend on the proportion of fast and slow fibres that affect the curvature and maximum shortening velocity (eqns. 6-8). Two sets of estimates for v_0 were used. The first set was calculated from the twitch rise times for the goats. It is possible that these underestimated v_0 due to experimental challenges of detecting motor unit twitch dynamics from whole muscle twitches (Lee et al. 2011), and that they were predicted by extrapolation from a relation that was derived from smaller species (eqn. 1). A second set of greater values for v_0 was chosen to bracket the expected range of v_0 that likely occurred in these muscles. From the ANOVA, the model outputs were not sensitive to the choice of the fibre-type proportion, but were sensitive to the choice of v_0. A possible explanation is as follows: despite the limb being held isometrically in a stereotactic frame, the fibres showed oscillations in length and velocity due to elastic compliance within the muscle-tendon-unit. The force-length and force-velocity properties of the muscle thus modulated the predicted muscle

force. The force-velocity modulation is greatest when the absolute velocity is a greater proportion of v_0 (eqns. 4-5). Thus, models with higher values of v_0 showed smaller force modulations due to the reduced force-velocity effect, and this resulted in better fits to the measured forces. Models A-D differed in their predictions of muscle forces despite having the same activation profiles. This further demonstrates that the models were sensitive to the force-velocity properties that were used.

During the trains of stimuli there were fluctuations in the muscle force that were not a function of systematic processes, such as fatigue. These fluctuations occurred despite a constant stimulus voltage, indicating that the force was not always maximal and thus not all the motor units were activated for each twitch. This interpretation is consistent with our findings that the maximal muscle forces measured from these goats *in vivo*, during nearly isometric phases of contraction, exceeded the muscle forces that we could elicit *in situ* (de Boef Miara, personal communication). Our nerve-cuff design and implementation evolved and improved throughout the study; nonetheless, the recorded data do show fluctuations in motor unit recruitment. These fluctuations enabled this study, since they allowed the alternative models of motor recruitment to be tested on these data. Had all the motor units been recruited for each stimulus, then this evaluation of the different models would not have been possible.

The models predicted force more accurately for the goat LG than for the MG (Figs. 4,5), perhaps due to variations in the muscle architecture and the intrinsic properties of the motor units. For example, differences in the fascicle rotation may have contributed to minor differences in performance. It was assumed that the effect of fascicle rotations could be ignored, since the only evidence for fascicle rotations during contraction in the LG and MG comes from man, where differences between the muscles are less than 5° (Maganaris et al. 1998; Wakeling et al. 2011). It is interesting to consider that if the muscles had been less pennate, or even parallel-

fibred, in architecture that the fibre rotations during contraction would have been less, or even non-existent, and so the models would have the potential to better predict the tendon force. Differences in the motor unit twitch profiles between the LG and MG in both man and goats have also been reported in previous studies (Vandervoort and McComas, 1983; Lee et al. 2011) and may reflect differences in activation-relaxation dynamics that affect the accuracy of the predicted muscle force.

Motor unit recruitment and the differential muscle model

Muscle models used for biomechanical simulations typically assume an orderly recruitment of motor units, based on classic neurophysiological studies (Henneman et al. 1974). However, different types of motor units can be differentially activated for different mechanical tasks (Gillespie et al. 1974; Hoffer et al. 1981; Loeb 1985; Wakeling, 2004). It has been suggested, for example, that faster fibres may be utilized for power production at high contraction speeds (Rome et al. 1988). Indeed, we have previously shown that the recruitment of faster fibres significantly correlates with the strain rates of the fibres in both rats and man (Wakeling et al. 2006; Hodson-Tole and Wakeling, 2008b). It has also been suggested that faster fibres are recruited for contractions that require fast rates of force development and relaxation (Biewener et al. 1992; Hodson-Tole and Wakeling, 2008a; Roberts and Gabaldón, 2008).

There was fluctuation in the motor recruitment patterns during *in situ* stimulations, despite the constant nerve excitation. These produced fluctuations in the activity levels of the different motor units, and these features were only captured in the activation input to differential model E. The fluctuations in recruitment were not apparent from the raw EMG or the total intensity traces, but were only apparent after the EMG signals had been resolved into their time-frequency components (Fig. 6). This illustrates the utility of the wavelet techniques for identifying patterns of motor recruitment from the EMG. The ability of differential model E to

respond to the activation dynamics of the different types of motor units resulted in improved model performance. The sensitivity of the models to the activation-relaxation dynamics is illustrated by the fact that the models show a poorer fit where the stimulation rates are low (Fig. 4, 5) and where the activation dynamics are more important; this result parallels similar observations in the cat soleus (Perreault et al. 2003). Differential model E showed the greatest improvement relative to the traditional models at the lowest stimulation frequencies (Fig. 4) due to its enhanced ability to predict the activation-dependant fluctuations from the different motor units.

Conclusion

This study showed that a muscle model comprised of parallel fast- and slow components that could be independently activated generated better predictions of whole muscle force than traditional Hill-type models (eg. Fig. 2). This *in situ* study examined the muscle forces during contractions that were isometric for the muscle-tendon unit, where the fibre strains and strain rates may be much more limited than during free movement. These contractions form a particularly challenging data set with which to discriminate among the different models because they would have involved limited fascicle velocities. By contrast, we would expect a larger change in recruitment patterns to exist across a range of locomotor behaviours *in vivo* (Hodson-Tole and Wakeling, 2009) and this is where models that accommodate varying recruitment may perform substantially better. Nonetheless, the differential model performed the best in this study and demonstrated that motor unit recruitment is an important feature of muscle force. This is to be expected, but has largely been ignored in prior implementation of Hill-type muscle models. We expect that even greater improvements in muscle force prediction will be realized when the models are compared over a wide range of locomotor tasks *in vivo*.

7. Acknowledgements

8. References

1. Ariano, M.A., R.B. Armstrong, and V.R. Edgerton. Hindlimb muscle fiber populations of five mammals. J. Histochem. Cytochem. 21: 51-55,1973.

2. Askew G.N. and R.L. Marsh. Optimal shortening velocity (V/Vmax) of skeletal muscle during cyclical contractions: length-force effects and velocity-dependent activation and deactivation. J. Exp. Biol. 201: 1527-1540, 1998.

3. Askew, G.N. and R.L. Marsh. The effects of length trajectory on the mechanical power output of mouse skeletal muscles. J. Exp. Biol. 200: 3119-3131, 1997.

4. Balnave C.D. and D.G. Allen. The effect of muscle length on intracellular calcium and force in single fibres from mouse skeletal muscle. J. Physiol. 492: 705-713, 1996.

5. Biewener, A.A., K.P. Dial, and G.E. Goslow. Pectoralis muscle force and power output during flight in the starling. J. Exp. Biol. 164: 1-18, 1992.

6. Böl, M., M. Sturmat, C. Weichert and C. Kober. A new approach for the validation of skeletal muscle modelling using MRI data. Comput. Mech. 47, 591-601, 2011.

7. Bottinelli, R. and C. Reggiani. Human skeletal muscle fibres: molecular and functional diversity. Prog. Biophys. Mol. Biol. 73: 195-262, 2000.

8. Brown I.E., E.J.Cheng, and G.E. Loeb. Measured and modeled properties of mammalian skeletal muscle. II. The effects of stimulus frequency on force-length and force-velocity relationships. J Muscle Res Cell Motil 20: 627-643, 1999.

9. Buchanan, T.S., D.G. Lloyd, K. Manal, and T.F. Besier. Neuromusculoskeletal modelling: estimation of muscle forces and joint moments and movements from measurements of neural command. J. Appl. Biomech. 20: 367-395, 2004.

10. Buller, A.J., C.J.Kean, and K.W. Ranatunga. Transformation of contraction speed in muscle following cross-reinnervation; dependence on muscle size. J. Muscle. Res. Cell Motil. 8: 504-516, 1987.

11. Burke, R.E., D.N. Levine, F.E. Zajac, P. Tsairis, and W.K. Engel. Mammalian motor units: physiological-histochemical correlation in three types in cat gastrocnemius. Science 174: 709-712, 1971.

12. Close, R.I. The relations between sarcomere length and characteristics of isometric twitch contractions of frog sartorius muscle. J Physiol 220: 745-762, 1972.

13. Close, R.I. Dynamic properties of fast and slow skeletal muscles of the rat during development. J. Physiol. 173: 74-95, 1964.

14. Close, R.I. Force: velocity properties of mouse muscles. Nature 206: 718-719, 1965.

15. Close, R.I. Dynamic properties of mammalian skeletal muscles. Physiol. Rev. 52: 129-197, 1972.

16. Close, R.I. and A.R. Luff. Dynamic properties of inferior rectus muscle of the rat. J. Physiol. 236: 259-270, 1974.

17. Edwards, R.H.T. Human muscle function and fatigue. In Human muscle fatigue: physiological mechanisms. R. Porter & J. Whelan eds. Pitman Medical, London, pp1-18, 1981.

18. Epstein, M. and W. Herzog. Theoretical models of Skeletal muscle, John Wiley & Sons, New York, 238pp, 1998.

19. Farina D, M. Fosci and R. Merletti Motor unit recruitment strategies investigated by surface EMG variables. J. Appl. Physiol. 92: 235-247, 2002.

20. Fuglevand, A.J., D.A. Winter and A.E. Patla. Models of recruitment and rate coding organization in motor-unit pools. J. Neurophysiol. 70, 2470-2488, 1993.

21. Gillespie, C.A., D.R. Simpson, and V.R. Edgerton. Motor unit recruitment as reflected by muscle fibre glycogen loss in a prosimian (bushbaby) after running and jumping. J Neurol Neurosurg Psychiatry 37: 817-824, 1974.

22. Gillis, G.B., J.P. Flynn, P. McGuigan, and A.A. Biewener. Patterns of strain and activation in the thigh muscles of goats across gaits during level locomotion. J. Exp. Biol.

208: 4599-4611, 2005.

23. Henneman, E., H.P. Clamann, J.D. Gillies, and R.D. Skinner. Rank order of motorneurones within a pool, law of combination. J. Neurophysiol. 37: 1338-1349, 1974.

24. Hernandez, A., A.L. Lenz, and D.G. Thelen. Electrical stimulation of the rectus femoris during pre-swing diminishes hip and knee flexion during the swing phase of normal gait. *IEEE Trans. Neural Sys. Rehab. Eng.* 18(5): 523-530, 2010.

25. Hill, A.V. First and last experiments in muscle mechanics. Cambridge University Press, 1970.

26. Hodson-Tole, E., and J.M. Wakeling. Variations in motor unit recruitment patterns occur within and between muscles in the running rat (Rattus norvegicus). J. Exp. Biol. 210: 2333-2345, 2007.

27. Hodson-Tole, E., and J.M. Wakeling. Motor unit recruitment patterns 1: Responses to changes in locomotor velocity and incline. J. Exp. Biol. 211: 1882-1892, 2008a.

28. Hodson-Tole, E., and J.M. Wakeling. Motor unit recruitment patterns 2: The influence of myoelectric intensity and muscle fascicle strain rate. J. Exp. Biol. 210, 211: 1893-1902, 2008b.

29. Hodson-Tole, E., and J.M. Wakeling. Motor unit recruitment for dynamic tasks: current understanding and future directions. J. Comp Physiology B. 179: 57-66, 2009.

30. Hodson-Tole, E., and J.M. Wakeling. The influence of strain and activation on the locomotor function of rat ankle extensor muscles. J. Exp. Biol. 213: 318-330, 2010.

31. Hoffer, J.A., M.J. O'Donovan, C.A. Pratt, and G.E. Loeb. Discharge patterns of hindlimb motoneurons during normal cat locomotion. Science 213: 466-467, 1981.

32. Johnson, M.A., J. Polgar, D. Weightman, and D. Appleton. Data on the dirtribution of fibre types in thirty-six human muscles. An autopsy study. J. Neurol. Sci. 18: 111-129, 1973.

33. Lee, S.S.M., M. de Boef Miara, A. Arnold-Rife, A.A. Biewener, and J.M. Wakeling. EMG analysis tuned for determining the timing and level of activation in different motor units. J. Electromyogr. Kinesiol. 21: 557–565, 2011.

34. Loeb, G.E. Motoneurone task groups: coping with kinematic heterogeneity. J Exp Biol 115: 137-146, 1985.

35. Luff, A.R. Dynamic properties of fast and slow skeletal muscles in the cat and rat following cross-reinnervation. J. Physiol. 248: 83-96, 1975.

36. Luff, A.R. Dynamic properties of the inferior rectus, extensor digitorum longus, diaphragm and soleus muscles of the mouse. J. Physiol. 313:161-171, 1981.

37. Maganaris, C.N., V. Baltzopoulos, and A.J. Sargeant. In vivo measurements of the triceps surae complex architecture in man: implications for muscle function. J Physiol 512: 603-614, 1998.

38. McGuigan, M.P., E. Yoo, D.V. Lee, and A.A. Biewener. Dynamics of goat distal hind limb muscle-tendon function in response to locomotor grade. J. Exp. Biol. 212: 2092-2104, 2009.

39. Otten, E. A myocybernetic model of the jaw system of the rat. J. Neurosci. Methods 21: 287-302, 1987a.

40. Otten, E. Optimal design of vertebrate and insect sarcomeres. J Morphol 191: 49-62, 1987b

41. Perreault, E.J., C.J. Heckman, and T.G. Sandercock. Hill muscle model errors during movement are greatest within the physiologically relevant range of motor unit firing rates. J. Biomech. 36: 211-218, 2003.

42. Rack, P.M.H. and D.R. Westerbury. The effects of length and stimulus rate on tension in the isometric cat soleus muscle. J. Physiol. 204: 443-460, 1969.

43. Ranatunga, K.W. Temperature-dependence of shortening velocity and rate of isometric tension development in rat skeletal muscle. J. Physiol. 329: 465-483, 1982.

44. Rassier, D.E., W. Herzog, J. Wakeling, and D.A. Syme. Stretch-induced, steady-state force enhancement in single skeletal muscle fibers exceeds the isometric force at optimum fiber length. J. Biomech 36: 1309-1316, 2003.

45. Roberts, T.J. and A.M. Gabaldón. Interpreting muscle function from EMG: lessons learned from direct measurements of muscle force. Int. Comp. Biol. 48: 312-320, 2008.

46. Roszek, B., G.C. Baan, and P.A. Huijing. Decreasing stimulation frequency-dependent length-force characteristics of rat muscle. J Appl Physiol 77: 2115-2124, 1994.

47. Solomonow, M. External control of the neuromuscular system. IEEE Trans. Biomed. Eng. 31: 752-763, 1984.

48. Spector, S.A., P.F. Gardiner, R.F. Zernicke, R.R. Roy, and V.R. Edgerton. Muscle

architecture and force-velocity characteristics of cat soleus and medial gastrocnemius: implications for motor control. J. Neurophysiol. 44: 951-960, 1980.

49. Stephenson, D.G. and I.R. Wendt. Length dependence of changes in sarcoplasmic calcium concentration and myofibrillar calcium sensitivity in striated muscle fibres. J. Mus. Res. Cell Mot. 5: 243-272, 1984.

50. Tanner, J.A. Reversible blocking of nerve conduction by alternating-current excitation. Nature 195, 712-713, 1962.

51. Toniolo, L., M. Patruno, L. Maccatrozzo, M.A. Pellegrino, M. Canepari, R. Rossi, G. D'Antona, R. Bottinelli, C. Reggiani, and F. Mascarello. Fast fibres in a large animal: fibre types, contractile properties and myosin expression in pig skeletal muscles. J. Exp. Biol. 207: 1875-1886, 2004

52. Umberger, B.R., K.G.M. Gerritsen, and P.E. Martin. A model of human muscle energy expenditure. Comput. Meth. Biomech. Miomed. Eng. 6: 99-111, 2003.

53. Van Leeuwen, J.L. Muscle function in locomotion. In Mechanics of Animal Locomotion (ed. R.McN. Alexander) pp 191-250, 1992.

54. Van Soest, A.J. and M.F. Bobbert. The contribution of muscle properties in the control of explosive movements. Biol. Cybernetics 69: 195-204, 1993.

55. Vandervoort, A.A., and A.J. McComas. A comparison of the contractile properties of the human gastrocnemius and soleus muscles. Eur. J. Appl. Physiol. 51: 435-440, 1983.

56. von Tscharner, V. Intensity analysis in time-frequency space of surface myoelectric signals by wavelets of specified resolution. J. Electromyogr. Kinesiol. 10: 433-445, 2000.

57. Wakeling, J.M., K. Uehli, and A.I. Rozitis. Muscle fibre recruitment can respond to the mechanics of the muscle contraction. Journal of the Royal Society Interface 3:533-544, 2006.

58. Wakeling, J.M. Motor units are recruited in a task dependent fashion during locomotion. J. Exp. Biol. 207: 3883-3890, 2004.

59. Wakeling J.M. Patterns of motor recruitment can be determined using surface EMG. J. Electromyogr. Kinesiol. 19: 199-207, 2009.

60. Wakeling, J.M., O.M. Blake, I. Wong, M. Rana, and S.M.M. Lee. Movement mechanics

as a determinate of muscle structure, recruitment and coordination. Phil. Trans. Roy. Soc. B 366: 1554-1564, 2011.

61. Wakeling, J.M., M. Kaya, G.K. Temple, I.A. Johnston, and W. Herzog. Determining patterns of motor recruitment during locomotion. J. exp. Biol. 205: 359-369, 2002.

62. Wakeling, J.M., and D.A. Syme. Wave properties of action potentials from fast and slow motor units. Muscle Nerve 26: 659-668, 2002.

63. Winters, J.M. and L. Stark. Estimated mechanical properties of synergistic muscles involved in movements of a variety of human joints. J. Biomech. 21: 1027-1041, 1988.

64. Winters, T.M., M. Takahashi, R.L. Lieber, and S.R. Ward. Whole muscle length-tension relationships are accurately modeled as scaled sarcomeres in rabbit hindlimb muscles. J. Biomech. 44: 109-115, 2011.

65. Zajac, F.E. Muscle and tendon: properties, models, scaling, and application to biomechanics and motor control. Crit. Rev. Biomed. Eng. 17, 359-411, 1989.

9. Tables

Table 1. parameters used in the equations for the muscle models

Parameter	Definition	Source
$\hat{a}(t)$	activation state of fibres	derived from measured EMG (Lee et al. 2011)
c_1	scalar to calculate actual from normalized force	measured
c_2/c_3	ratio scales activation between fast and slow components	calculated
F_m	muscle force	calculated
$\hat{F}_p(l)$	normalized, passive force-length relation	measured
$\hat{F}_a(l)$	normalized, active force-length relation	measured
$\hat{F}(v)$	normalized, force-velocity relation	literature
k	curvature of force-velocity relation	literature
l	fascicle length	measured
v	fascicle velocity	derived from l
v_0	maximum shortening velocity	literature
β	pennation	measured
τ_a	force-rise time	measured (Lee et al. 2011)

subscripts "fast" and "slow" denote that parameters are specific to the fast or slow compartments in the differential model

Table 2. Key parameters used in the five muscle models.

Model	Force-velocity curvature, k	Maximum unloaded shortening velocity, v_0	Activation state
Homogeneous, A	$k_{\text{slow}} + (k_{\text{fast}} - k_{\text{slow}})p$	$v_{0,\text{fast}}\, p + v_{0,\text{slow}}(1-p)$	$\hat{a}(t)$
Hybrid, B	Composite from Hill (1970)	$v_{0,\text{fast}}$	$\hat{a}(t)$
Orderly, C	$k_{\text{slow}} + (k_{\text{fast}} - k_{\text{slow}})p$	$v_{0,\text{slow}} + (v_{0,\text{fast}} - v_{0,\text{slow}})\hat{a}(t)$	$\hat{a}(t)$
Reverse, D	$k_{\text{slow}} + (k_{\text{fast}} - k_{\text{slow}})p$	$v_{0,\text{fast}} - (v_{0,\text{fast}} - v_{0,\text{slow}})\hat{a}(t)$	$\hat{a}(t)$
Differential, E	k_{fast}	$v_{0,\text{fast}}$	$\hat{a}_{\text{fast}}(t)$
	k_{slow}	$v_{0,\text{slow}}$	$\hat{a}_{\text{slow}}(t)$
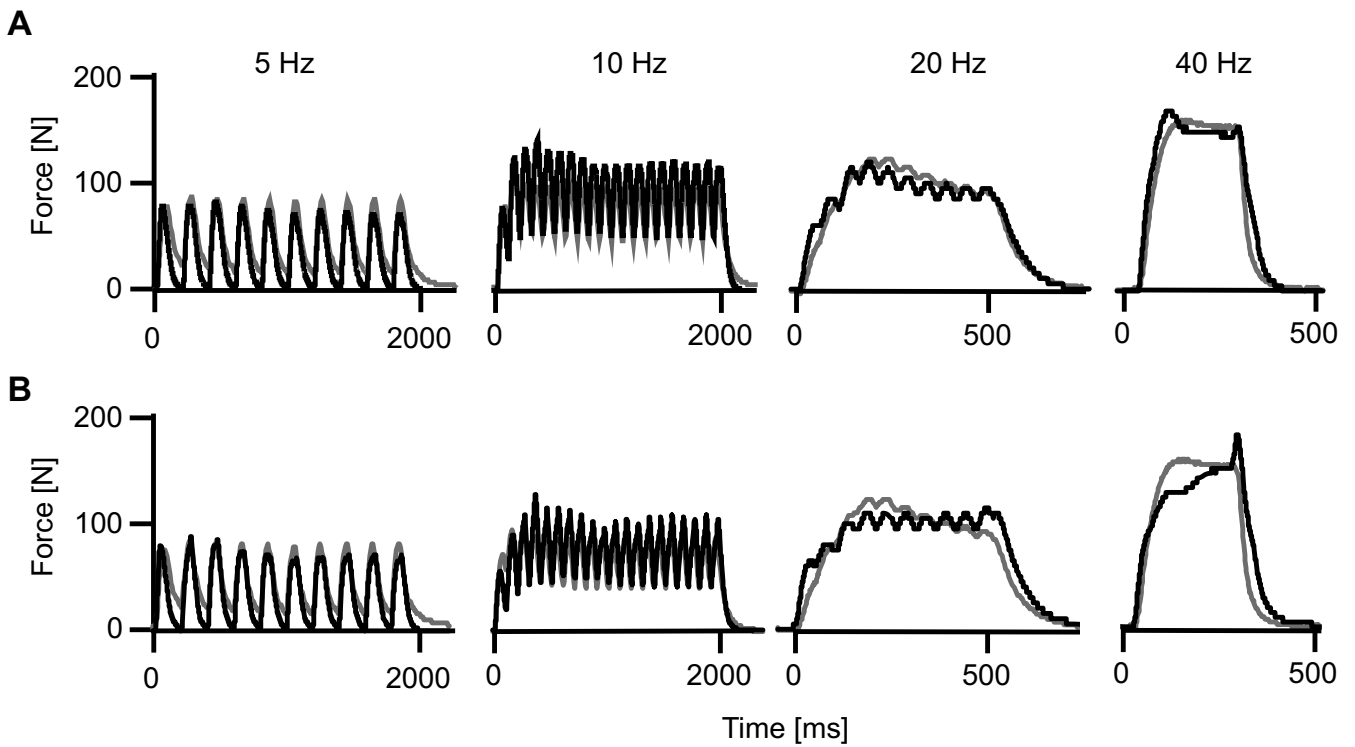
Fig. 1. Composite traces of muscle force for a series of contractions in the medial gastrocnemius at a range of stimulation frequencies. Measured forces are shown in grey, and predicted forces are shown in black. The forces were modelled using differential model E, with v_0 estimated at 5 and 10 s^{-1} (A) or 2.74 and 3.59 s^{-1} (B) for the slow and fast-fibres, respectively, and with fast fibres comprising 75 % of the muscle.
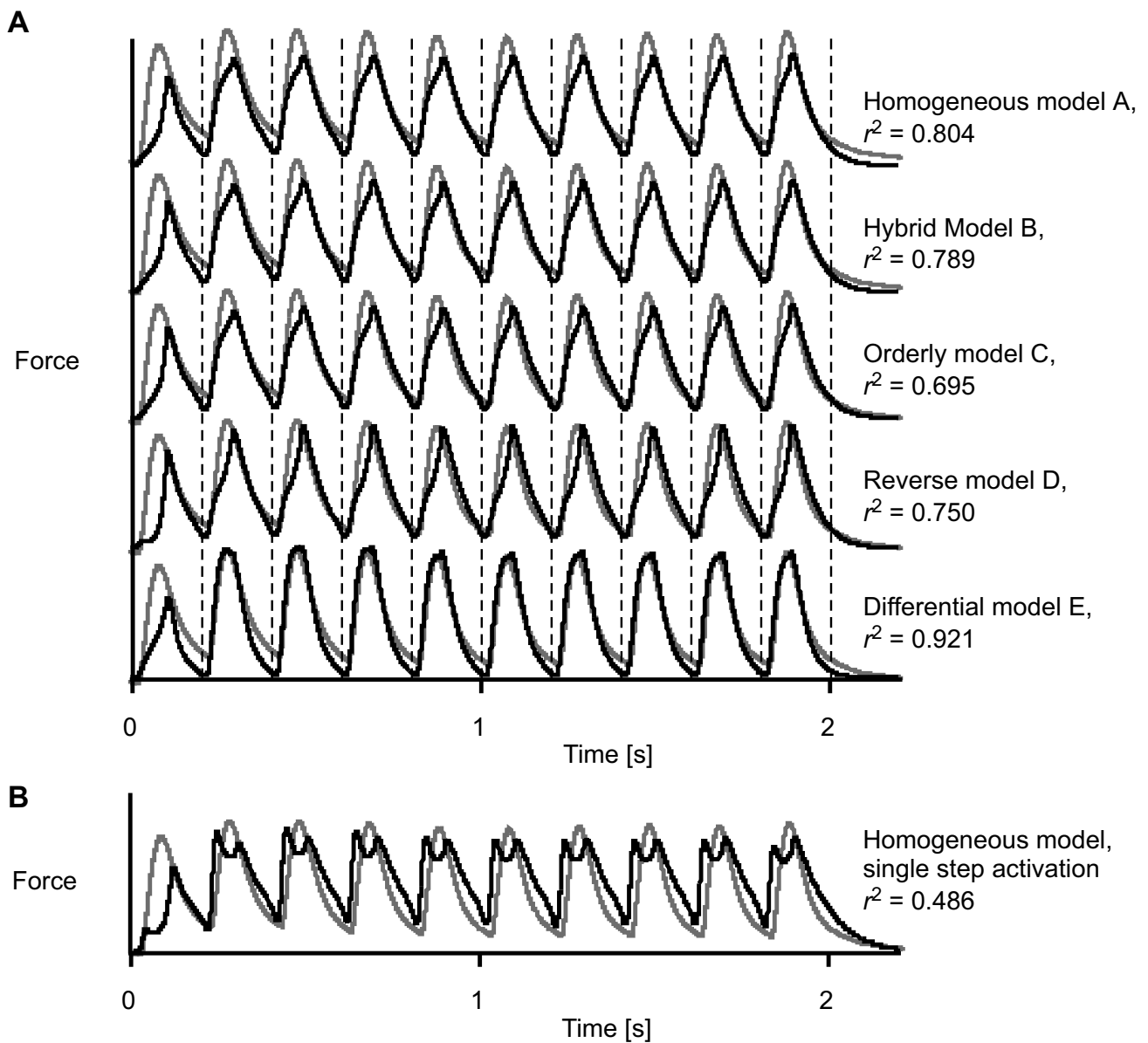
Fig. 2. Forces for a 5 Hz train of twitches in the medial gastrocnemius, calculated using different muscle models. Models A-E are shown in panel A. For comparison, a homogeneous model using a single-step first-order ordinary differential equation was used to calculate the activation is shown in panel B. Measured tendon forces are shown in grey, and predicted forces are shown in black. Vertical lines show the times of each stimulus. The forces were modelled with v_0 estimated at 5 and 10 s^{-1} for the slow and fast-fibres, respectively, and with fast fibres comprising 75 % of the muscle. The coefficient of determination, r^2, is shown for each model with respect to the measured force.
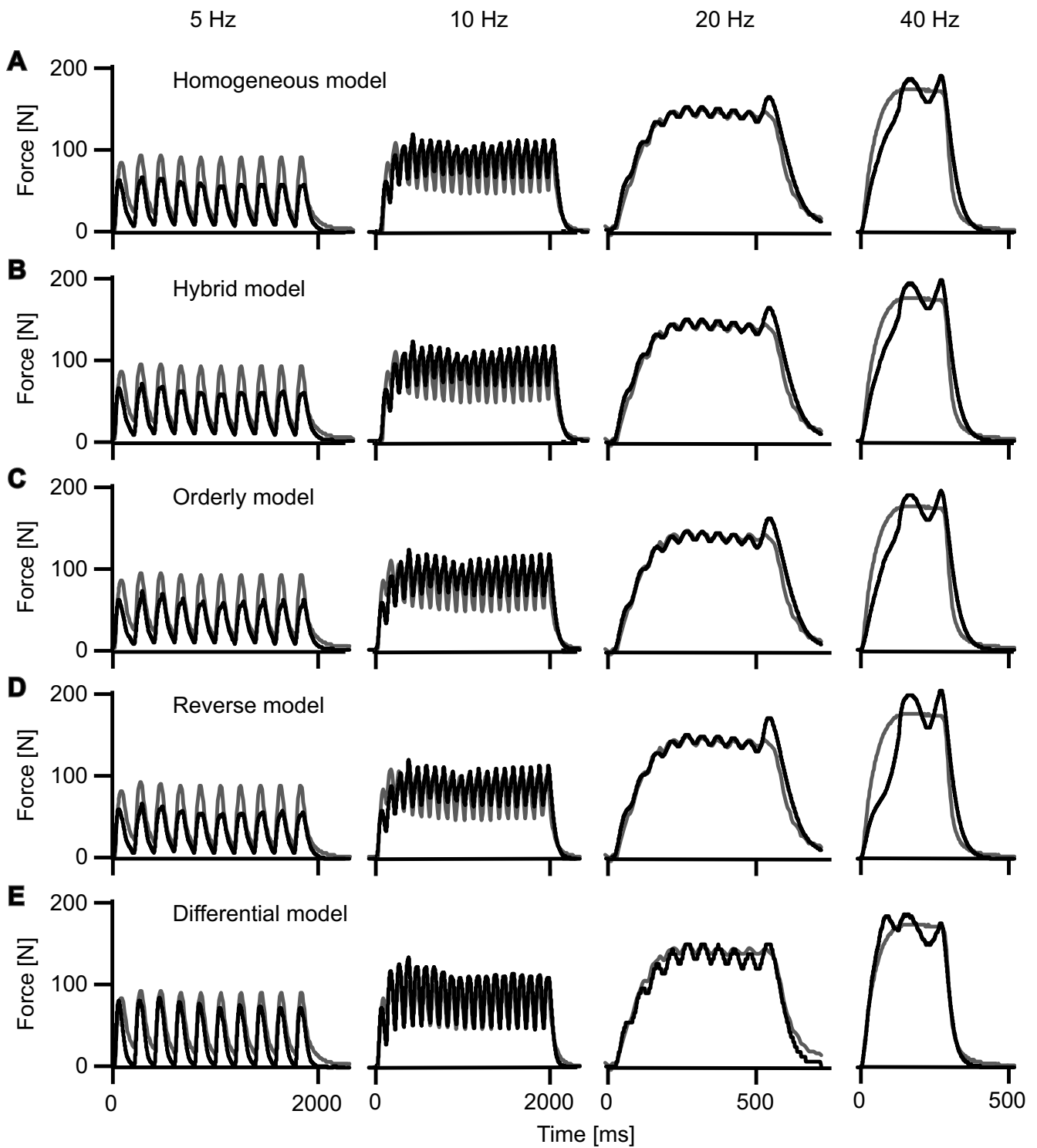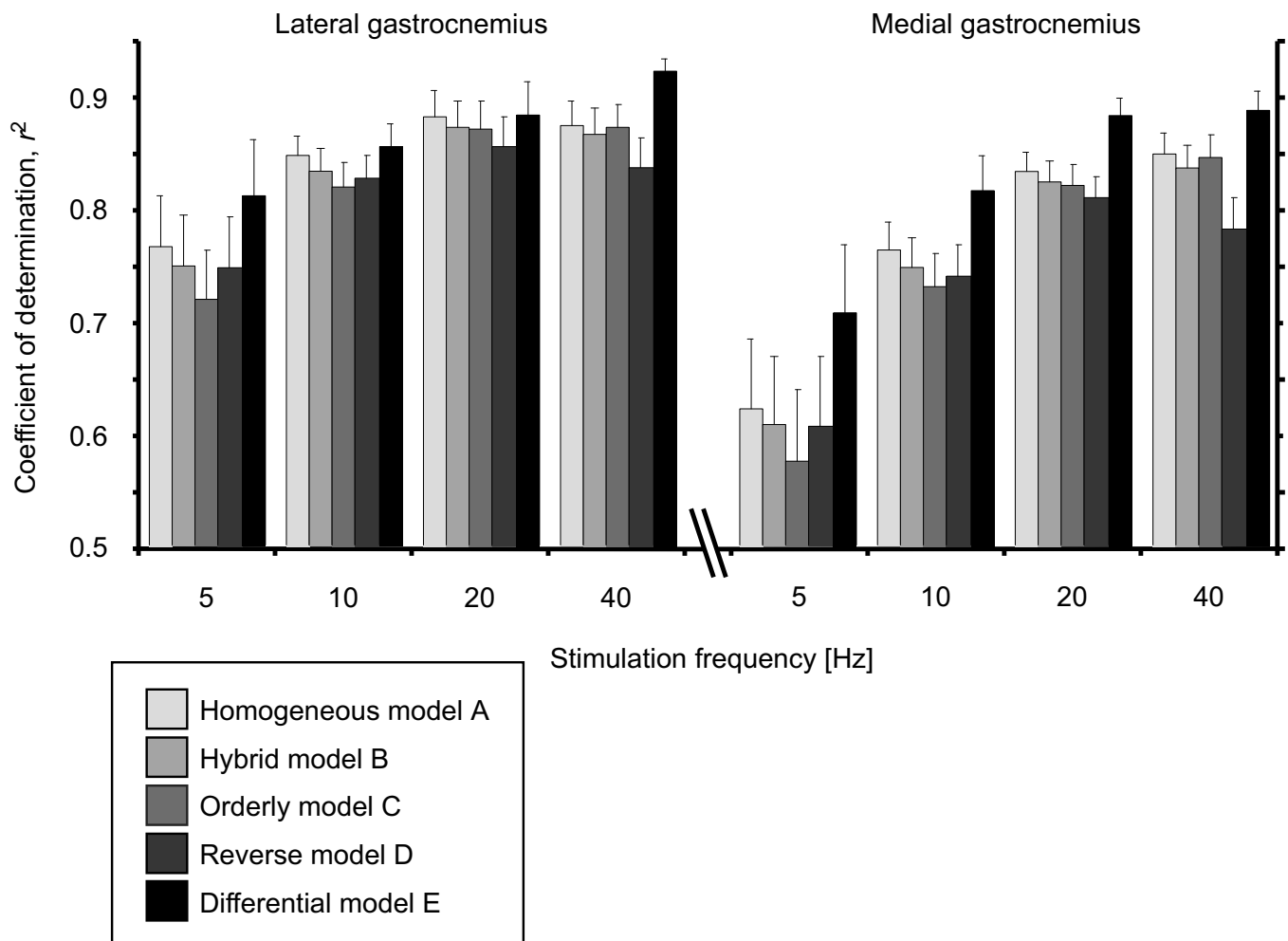
Fig. 3. The performance of the different muscle models across a range of stimulation frequencies for the lateral gastrocnemius. Measured tendon forces are shown in grey, and predicted forces are shown in black. The forces were modelled with v_0 estimated at 5 and 10 s^{-1} for the slow and fast-fibres, respectively, and with fast fibres comprising 75 % of the muscle.

Fig. 4. The performance of the different muscle models for the different stimulation frequencies and muscles. Bars show the mean + s.e.m. values (*N*=20) pooled from the different goats, fibre-type proportions and choices of v_0.
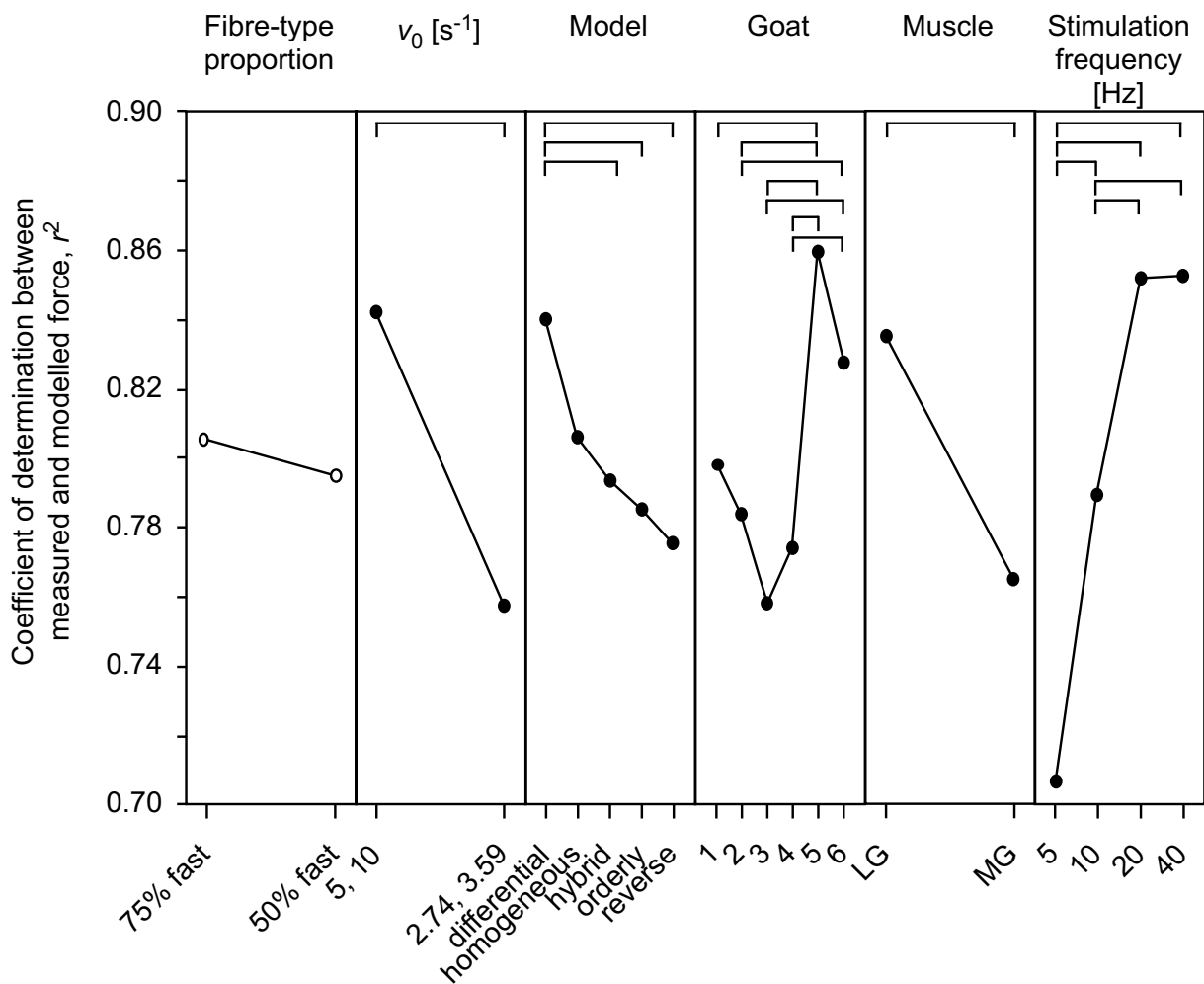
Fig. 5. The main effects of model parameters and experimental factors on the coefficient of determination. Points show the main effects (least-squares adjusted means) from the ANOVA. Where a factor had a significant effect on the coefficient of determination the points are shown by filled circles, open circles denote no significant effect. Post-hoc Tukey tests identified specific differences within each category, and they are denoted by the horizontal bars.
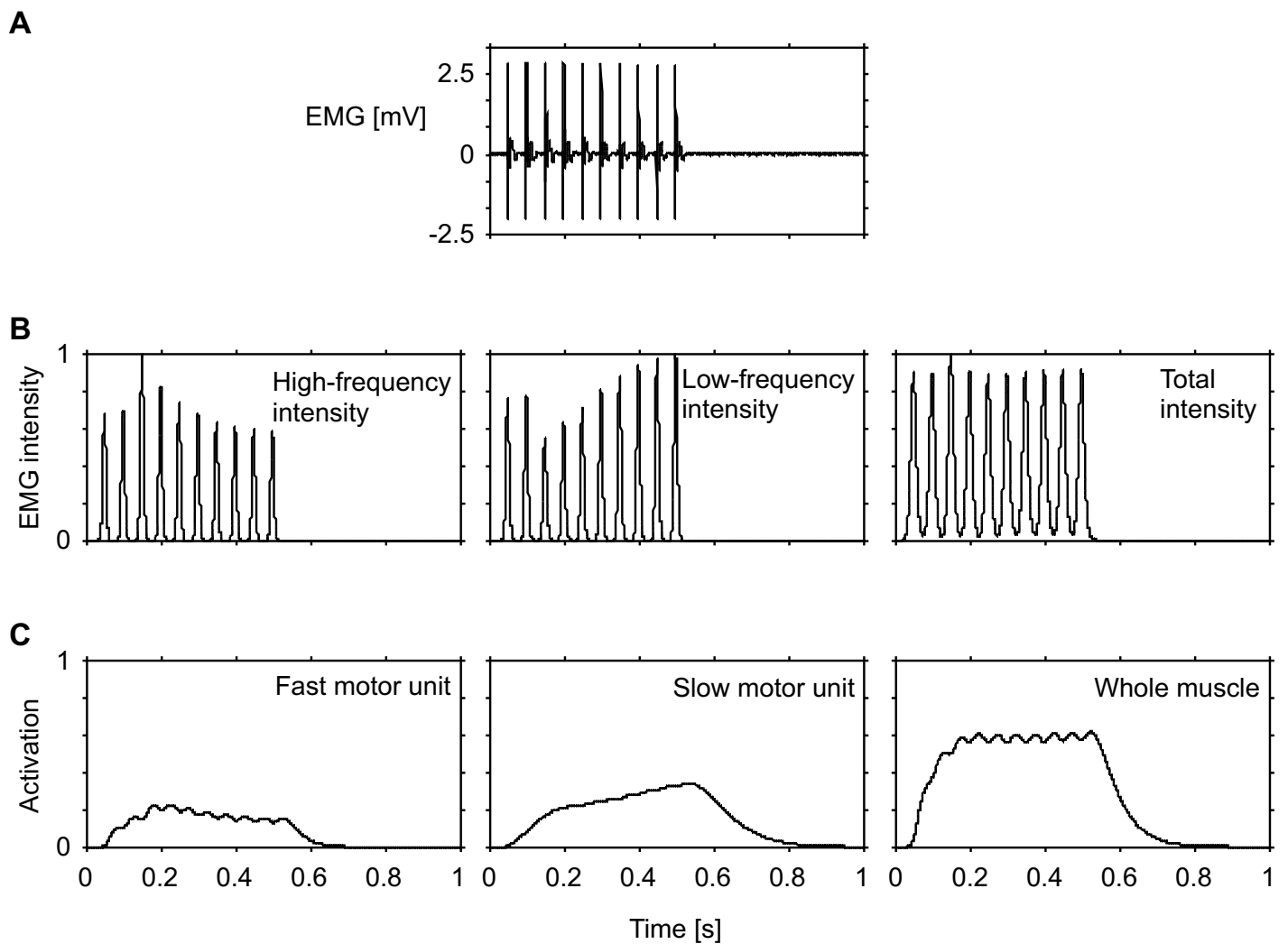
Fig. 6. EMG and activation states for the medial gastrocnemius muscle during a tetanic contraction stimulated at 20 Hz. EMG intensity is shown for the high (240.5 to 422.9 Hz) and low (82.4 to 247.0 Hz) frequency bands, corresponding to the fast- and slow- motor unit activity, respectively (B). The intensities were normalized to their maximum values during these supramaximal stimuli. The activation profiles are shown for the fast- and slow- motor units, and for the whole muscle (C).